Improved Energy Conversion for Doubly Fed Wind Generators

Alexander C. Smith, *Senior Member, IEEE*, Rebecca Todd, Mike Barnes, *Member, IEEE*, and Peter J. Tavner

***Abstract*—There is currently significant interest in offshore wind turbines up to 5 MW. One of the preferred options is doubly fed slip-ring generators. Turbine manufacturers have proposed an operating scheme for low speeds that is claimed to improve the overall energy extraction from the wind. This paper aims to examine the performance benefits for this new operational mode on a small experimental rig, confirmed by simulation, and to provide a fundamental understanding of the differences in the generator operation in both modes. This paper develops analytical steady-state models to provide this insight and correlates the operating performance with a dynamic real-time generator control scheme and experimental results obtained from a laboratory test machine. A theoretical study on a 2-MW commercial turbine is also undertaken.**

***Index Terms*—Doubly fed (DF) generator, induction generator (IG), slip-energy recovery, wind-turbine generator.**

I. Introduction

THERE IS an increasing demand for wind energy with the impetus coming from international legislation, environmental concerns, and the long-term availability of fossil fuels. International concern over climate change is resulting in political and regulatory pressure to reduce carbon-dioxide emissions, and many governments are actively seeking to increase the percentage share of the total electrical supply energy from renewable sources. Wind energy is viewed in this respect as a clean renewable source of energy, which produces no greenhouse-gas emissions or waste products. There are other sources of renewable energy, but wind energy is currently viewed as the lowest risk and most proven technology capable of providing significant levels of renewable energy in world terms. There has been a sustained effort over the past couple of decades to increase the power ratings of wind turbines at the same time improving their reliability and raising their availability. At present, 2–3-MW wind turbines are regarded as the standard, but the industry views 5 MW as the near-term target for single vertical turbines.

Paper IPCSD-06-071, presented at the 2005 Industry Applications Society Annual Meeting, Hong Kong, October 2–6, and approved for publication in the IEEE TRANSACTIONS ON INDUSTRY APPLICATIONS by the Electric Machines Committee of the IEEE Industry Applications Society. Manuscript submitted for review February 17, 2006 and released for publication July 1, 2006. This work was supported by the ERC Program of the National Science Foundation under Award EEC-9731677.

A. C. Smith, R. Todd, and M. Barnes are with the School of Electrical and Electronic Engineering, The University of Manchester, Manchester, M60 1QD, U.K. (e-mail: sandy.smith@manchester.ac.uk; rebecca.todd.@postgrad.manchester.ac.uk; mike.barnes@manchester.ac.uk).

P. J. Tavner is with the School of Engineering, University of Durham, Durham, DH1 3LE, U.K. (e-mail: Peter.Tavner@durham.ac.uk).

Digital Object Identifier 10.1109/TIA.2006.882640

As turbine power ratings have steadily increased, electrical generator technology has also adapted and developed from the early fixed-speed generators, in order to improve drive train dynamics and increase energy recovery. Modern vertical wind turbines are normally variable-speed units, and this requires the generator to be interfaced to the grid through an electronic power converter. Conventional generators such as induction or synchronous (permanent magnet or wound) options are viable, but these require the grid-side converter to be rated to match the generator. For very large wind turbines (> 2 MW, for example), these converters are complex and expensive at current prices. One of the preferred options at present therefore, for large turbines in excess of 2-MW rating, is the variable-speed doubly fed (DF) induction generator (IG) with the rotor converter connected to the rotor via slip rings [1]. This is in essence a slip-energy-recovery system, used for many years in large motor drives, taking direct advantage of the fact that limiting the speed range of the drive can reduce the rating of the converter and modern converter technology to improve the control of speed. Most wind turbines naturally restrict feasible operation to typically 30% above and below [2] the generator synchronous speed, and thus, a 3-MW wind turbine, for example, can operate with the stator connected directly to the grid and a 1-MW rotor-side converter to provide variable speed. This translates directly into significant cost savings for the rotor converter and also improves the overall reliability of the converter. The disadvantage of this option is the need for a slip-ring connection to the rotor, but this is still currently viewed as one of the preferred options for large wind turbines.

Modern DF turbine generators utilize a bidirectional pulsewidth-modulation (PWM) inverter that can control both the rotor voltage and phase angle so that the generator can operate at variable speed with control of the stator power factor over the nominal speed range [2]–[7]. As wind speeds fall, the generator output power reduces until the power extracted from the wind is insufficient to maintain the gear train and generator losses, and the generator would normally be disconnected from the grid at this point. Some commercial generator systems use star/delta-winding connections as one means of extending this speed range. Turbine manufacturers have recently proposed an operating scheme for low wind speeds that is claimed to improve the overall energy extraction and extend the operating speed range at which useful power can be extracted from the wind. The proposed operating scheme is to use a DFIG for normal wind conditions, but as the wind speed falls, the stator disconnects from the grid and short circuits it. The generator then reverts to a conventional IG mode of operation with all the power channeled through the rotor-side converter to the grid.

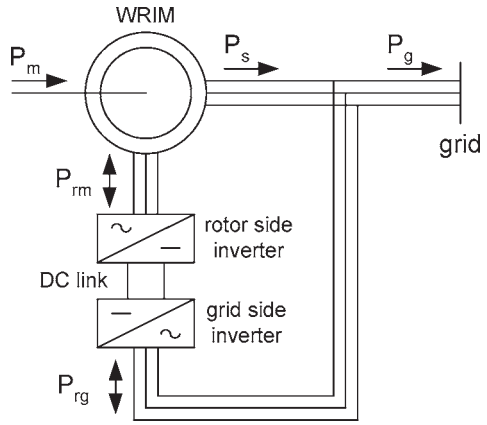

Fig. 1. DF connection.

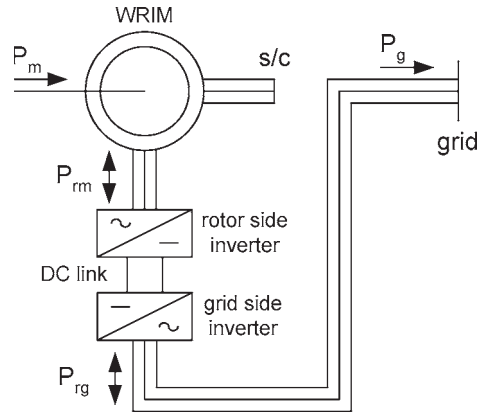

Fig. 2. IG connection.

The objective of this paper is to examine in detail the performance benefits for this new mode of wind-generator operation and to provide a fundamental understanding of the differences in the generator operation in both connections. This paper will utilize conventional steady-state equivalent circuits to provide this insight but will also correlate the operating performance with that obtained from the conventional closed-loop dynamic controller [8], [9]. This paper will also provide experimental results obtained from a laboratory test machine to validate the steady-state and dynamic simulations.

II. Generator—Double-Sided and Single-Sided Connections

Fig. 1 illustrates the conventional DF connection. Power flows into the rotor circuits via the rotor-side converter below synchronous speed and vice versa above synchronous speed. The grid-side inverter is typically controlled to maintain a constant dc link voltage, drawing unity power factor from the supply network [4]. The rotor-side inverter is controlled separately. The generator power factor can be controlled to provide reactive power and to regulate the local-grid voltage. However, operation at unity power factor is often desirable [10] when connected to lower voltage distribution networks to limit the level of plant upgrade needed.

Fig. 2 illustrates the IG connection. The stator windings are initially disconnected from the grid and are then short circuited as shown. In practice, the generator would be switched from one connection to the other using appropriate switchgear and switching-sequence control. The generator then behaves as a normal IG except that the rotor circuit now acts as the only grid connection through the rotor converter. This type of connection has occasionally been used in the past as a means of starting a DFIG.

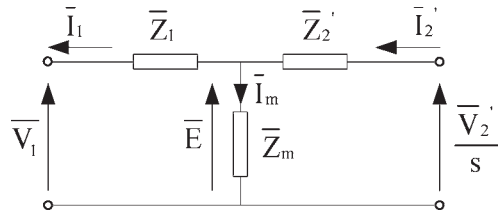

Fig. 3. Equivalent circuit for DFIG.

III. Steady-State Model

The standard steady-state per-phase equivalent circuit can be utilized for assessing the performance of both double-sided and single-sided connections subject to the usual assumptions of a three-phase balanced supply, fixed rotor speed, and constant machine parameters. Fig. 3 illustrates the conventional per-phase equivalent circuit for an IG in which the rotor circuits are referred to the stator frequency, so that all machine reactances are determined at supply frequency. This frequency transformation also scales the applied rotor voltage by the rotor slip, as shown in Fig. 3.

Solution of this equivalent circuit for the DF connection requires a search routine because there is more than one combination of rotor voltage and rotor phase angle that meets the known constraints of rotor speed, shaft torque, and stator rms voltage. The solution procedure starts from a power balance applied to the rotor.

The electrical power flowing into $(P_{\rm IN})$ and out $(P_{\rm OUT})$ of the rotor is defined as follows:

$$P_{\rm OUT}^{\rm R} = {\rm Re}\left\{3\overline{E}\bar{I}_2'^*\right\} \tag{1}$$

$$P_{\rm IN}^{\rm R} = {\rm Re}\left\{3\overline{V}'_2\bar{I}_2'^*\right\} \tag{2}$$

where the rotor voltages and currents are defined in Fig. 3. The rotor electrical losses are

$$P_{\rm LOSS}^{\rm R} = 3\left|\bar{I}_2'\right|^2 R_2' \tag{3}$$

where R_2' is the referred rotor resistance.

The only other power flow in or out of the rotor is the mechanical power defined as

$$P_{\rm IN}^{\rm R}({\rm mech}) = T\omega_r \tag{4}$$

where T is the generator torque, and $\omega_{\rm r}$ is the shaft speed.

Applying power balance to the rotor, we get

$$P_{\rm IN}^{\rm R} + P_{\rm IN}^{\rm R}({\rm mech}) = P_{\rm OUT}^{\rm R} + P_{\rm LOSS}^{\rm R} \tag{5}$$

or

$$\mathrm{Re}\left\{3\overline{V}'_2\bar{I}'^{*}_2\right\} + T\omega_r = \mathrm{Re}\left\{3\overline{E}\bar{I}'^{*}_2\right\} + 3\left|\bar{I}'_2\right|^2 R'_2. \quad (6)$$

This can be simplified by utilizing the circuit equations from Fig. 3

$$\overline{V}_1 + \bar{I}_1\overline{Z}_1 = \overline{E} \quad (7)$$

$$\frac{\overline{V}'_2}{s} = \bar{I}'_2\overline{Z}_2 + \overline{E}. \quad (8)$$

Rearranging (6)–(8), we get

$$T\omega_{\mathrm{s}} = \mathrm{Re}\left\{3\frac{\overline{V}'_2}{s}\bar{I}'^{*}_2\right\} - 3\left|\bar{I}'_2\right|^2\frac{R'_2}{s} \quad (9)$$

where ω_{s} is the synchronous speed.

This equation represents the basic torque equation for the DF generator. It also represents the starting point for the search routine to determine the required rotor voltage and phase angle. For any given wind speed, it is assumed that the known parameters are the shaft torque T, the generator speed, which defines the rotor slip s, and the rms grid voltage V_1. The objective is to determine the rotor voltage V'_2 and phase angle so that certain constraints are satisfied. The basic algorithm involves using the torque T and the rotor slip s to determine the rotor current I'_2 for any given rotor voltage and phase angle. The rotor current can then be used to determine the stator voltage V_1 and the stator current I_1. The first basic constraint that must be satisfied is the voltage V_1, which must equate to the grid voltage. Secondary constraints can then be added such as maximum rotor voltage and maximum rotor and stator currents. A final constraint can be included if the stator power factor needs to be controlled: The phase angle between V_1 and I_1 should be zero.

The initial step is to determine the rotor current from the shaft torque. This can be obtained from (9) in a straightforward manner if we use the rotor current as the reference phase angle in the equivalent circuit rather than the conventional supply voltage. The phase angles are therefore defined as follows:

$$\bar{I}'_2 = I'_2\angle 0 \quad \overline{V}'_2 = V'_2\angle\phi_2 \quad \overline{V}_1 = V_1\angle\phi \quad \bar{I}_1 = I_1\angle\phi_1.$$

Equation (9) reduces now to the solution of a simple quadratic equation

$$\left|\bar{I}'_2\right| = \frac{V'_2\cos\phi_2 - \sqrt{\left(V'_2\cos\phi_2\right)^2 - (4/3)R'_2Ts\omega_{\mathrm{s}}}}{2R'_2}. \quad (10)$$

Clearly, for a specified torque and slip, the rotor current can be determined for any rotor voltage V'_2 and phase angle ϕ_2. The air-gap electromovite force (EMF) E can then be obtained directly from (8) followed by the stator current I_1

$$\bar{I}_1 = \bar{I}'_2 - \frac{\overline{E}}{\overline{Z}_{\mathrm{m}}} \quad (11)$$

and, finally, the stator voltage V_1 from (7).

The final step in the algorithm is to check the constraints, and if these are satisfied, then the rotor voltage and phase angle represent a valid operating point for the DF generator.

The complete search algorithm can be summarized as follows.

1) Loop for all possible values of rotor voltage V'_2 and phase angle ϕ_2.
2) Determine rotor current I'_2 for specified torque and slip.
3) Calculate air-gap EMF E.
4) Determine the stator current I_1.
5) Determine the stator voltage V_1.
6) Check all constraints for valid rotor voltage V'_2 and phase angle ϕ_2.

The algorithm will index through all possible combinations of the rotor rms voltage and phase angle to find the values of V'_2 and ϕ_2 that ensures the stator voltage matches the grid voltage and also satisfies the additional constraints including the stator power factor, for example.

For the single-sided IG-connection mode, the solution of the conventional equivalent circuit is modified. The speed and torque are known, so the equivalent circuit can be used to determine the stator and rotor currents and hence the required rotor voltage V'_2 to sustain these. In the IG mode, the search variable is now the generator supply frequency. The constraints are also modified to include an additional check that the air-gap field does not exceed its rated value. This is normally determined by the air-gap EMF E divided by the supply frequency. The remaining constraints relate to maximum voltage and current ratings. The search routine, as before, determines the maximum generated output power and can be summarized as follows.

1) Loop for all possible values of rotor-converter frequency.
2) Determine stator current for specified torque and slip.
3) Calculate air-gap EMF E.
4) Determine the rotor current.
5) Determine the rotor supply voltage.
6) Check all constraints for valid rotor frequency.

IV. Transient-Generator Model and Control Strategy

On a practical wind turbine, the generator will have a real-time controller that will seek optimal performance under varying wind conditions. These are commonly based upon a field-orientated control algorithm [11] that uses power and stator reactive power as the reference parameters. The field-orientated control scheme incorporates a two-axis generator machine model and ensures that the generator operates at the reference points. To validate the steady-state algorithm described in the previous section, it is important to ensure that the dynamic real-time controller will produce the same operating point, as that determined by the steady-state model, by matching the control reference values to the performance constraints. The results therefore include the operating performance of the generator using a simulated real-time controller.

The control model used in this paper incorporates a conventional two-axis model of the DF machine into a field-orientated scheme orientated to the stator flux linkage [8], [11].

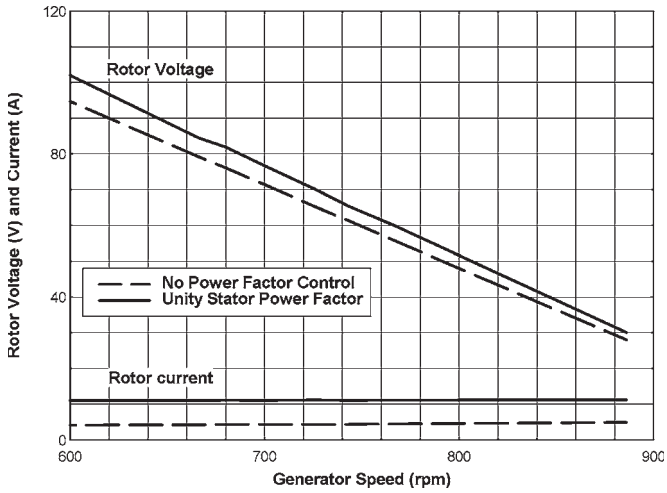

Fig. 4. DF connection (steady-state model).

The generator torque and stator power factor are used as the reference control parameters.

In the IG mode, a conventional field-orientated scheme [12]–[14] is also used, but it is adapted to reflect the fact that the converter supply is connected to the rotating rotor rather than a conventional-stator connection.

V. Experimental Test Generator

The analytical work described in the previous sections was validated using a small 7.5-kW six-pole wound-rotor test generator coupled to a dc motor on a laboratory test bed. A 15-kW bidirectional commercial converter was connected to the rotor slip rings. The real-time control scheme was created using MATLAB/SIMULINK and interfaced to the converter control processor using a dSPACE real-time development platform.

A detailed set of simulated results using both steady-state and dynamic control models was undertaken over a speed range from approximately 10% below synchronous speed (1000 r/min) to 40% below. Measured wind speed/power data from a commercial system were scaled and used to determine the generator torque for any given speed. Experimental results were recorded on the test generator in the IG-connection mode over the same speed range.

Fig. 4 illustrates the rotor voltage and current obtained using the steady-state model for the DF connection, with and without stator-power-factor control, over a speed range reducing from the normal generator synchronous speed of 1000 r/min. If no stator-power-factor control is required, the algorithm searches for the maximum generator efficiency by minimizing the winding copper losses. The efficiency of the rotor converter is not included in the search. It is clear from this figure that constraining the stator power factor results in a small increase in the rotor supply voltage but a more significant increase in the rotor current. This additional current has to be provided by the rotor converter and is needed to inject reactive power into the rotor to ensure unity stator power factor. The rotor current in both cases however remains relatively constant as the speed reduces. The rotor voltage on the other hand is determined mainly by the rotor speed and increases linearly as the rotor slip increases or speed reduces. This is an important factor in determining the rating of the rotor converter.

TABLE I
DF Mode—7.5 kW—Steady-State Equations (No pf Control)

Speed rpm	Stator Power W	Stator Power Factor	Grid Power W	Rotor Reactive Power VAr	Efficiency %
886	-1789.47	-0.36	-1549.37	334.13	95.41
766	-1331.27	-0.27	-982.92	660.01	93.57
743	-1246.48	-0.25	-891.05	714.46	93.05
726	-1191.08	-0.24	-828.85	765.79	92.63
700	-1100.94	-0.23	-735.05	837.31	91.89
680	-1038.47	-0.22	-669.19	901.83	91.24
666	-995.06	-0.21	-627.38	939.54	90.77
600	-794.55	-0.17	-442.06	1111.55	87.69

TABLE II
DF Mode—7.5 kW—Steady-State Equations (pf Control)

Speed rpm	Stator Power W	Grid Power W	Rotor Reactive Power VAr	Efficiency %
886	-1833.52	-1453.5	947.66	89.13
766	-1372.44	-883.32	1952.82	83.76
743	-1281.31	-785.97	2114.64	82.34
726	-1224.43	-719.62	2301.61	80.71
700	-1136.04	-628.79	2493.24	78.92
680	-1071.93	-561.86	2673.88	76.94
666	-1030.18	-522.28	2745.86	75.91
600	-834.042	-334.66	3341.46	66.78

Tables I and II summarize the power, reactive power, and efficiency values. Again, it is clear from these that there is a little change in the stator output power but a significant increase in the rotor reactive power for unity stator power factor. The stator power factor is relatively low in this generator when uncontrolled. The efficiency, on the other hand, is lower with power-factor control because of the additional losses caused by the extra current required to improve the power factor. In addition, it is evident that the efficiency begins to fall significantly with power-factor control as the speed reaches the lowest point in Table II. The efficiencies in general, however, are slightly high because only copper losses are included in the simulated results.

Fig. 5 illustrates the comparison between the steady-state results and those obtained using the real-time dynamic control model used in the laboratory generator.

It is clear that the correlation between the rotor voltage and current is excellent, confirming the validity of the steady-state approach in finding the optimum operating point. Table III summarizes the power, reactive power, and efficiency, and again, there is an excellent correlation with those obtained using the steady-state model in Table II. It confirms the capability of the steady-state approach described in this paper in undertaking detailed performance predictions for wind generators that would normally be operating under real-time dynamic control. The steady-state model will also act as a useful design tool for generator systems in wind-turbine applications.

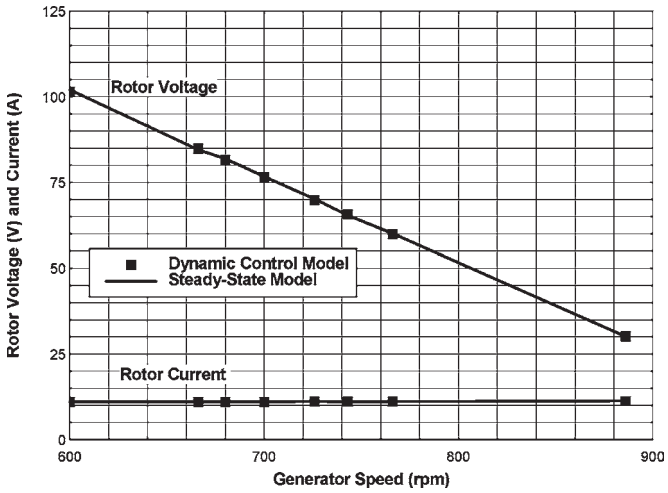

Fig. 5. DF connection with power-factor control.

TABLE III
DF MODE—7.5 kW—DYNAMIC CONTROL MODEL

Speed rpm	Stator Real Power W	Grid Real Power W	Rotor Reactive Power VAr	Efficiency %
886	-1798.71	-1425.70	950.55	89.17
766	-1361.45	-875.18	1940.19	83.65
743	-1280.62	-785.05	2134.73	82.29
726	-1238.47	-739.40	2279.85	81.98
700	-1131.74	-625.38	2490.04	78.79
680	-1054.63	-550.93	2655.07	76.70
666	-1017.58	-511.67	2763.08	75.34
600	-829.99	-334.99	3316.89	67.18

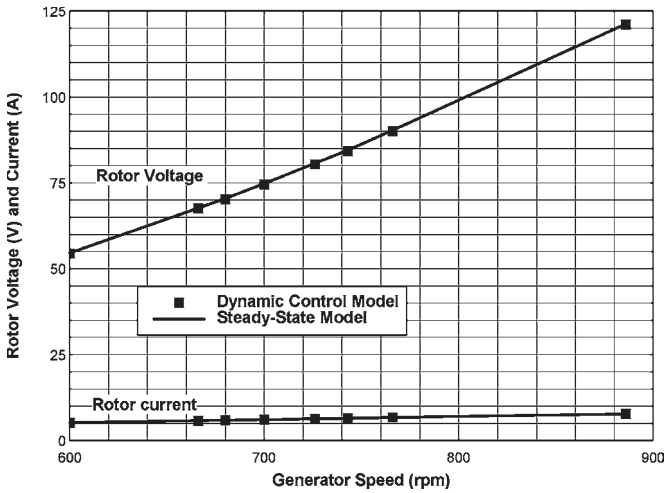

Fig. 6. IG-connection mode.

Fig. 6 illustrates the generator now reconnected in the IG mode over the same speed range. Again, there is a close correlation between the steady-state model and the simulated results using the dynamic control model implemented in the test generator. In this case, it is clear that the rotor current is close to that for the DF connection with no power-factor control. It is also evident that the search for maximum grid power results in a reducing rotor voltage as the speed reduces, which is in contrast to

TABLE IV
IG MODE—7.5 kW—STEADY-STATE EQUATIONS

Speed rpm	Grid Power W	Rotor Power Factor	Efficiency %
886	-1530.62	-0.54	93.86
766	-979.72	-0.54	92.90
743	-884.60	-0.54	92.68
726	-824.78	-0.54	92.51
700	-734.77	-0.54	92.22
680	-671.75	-0.54	91.99
666	-631.80	-0.54	91.83
600	-455.65	-0.53	90.93
533	-315.73	-0.53	89.79
400	-127.85	-0.52	86.39

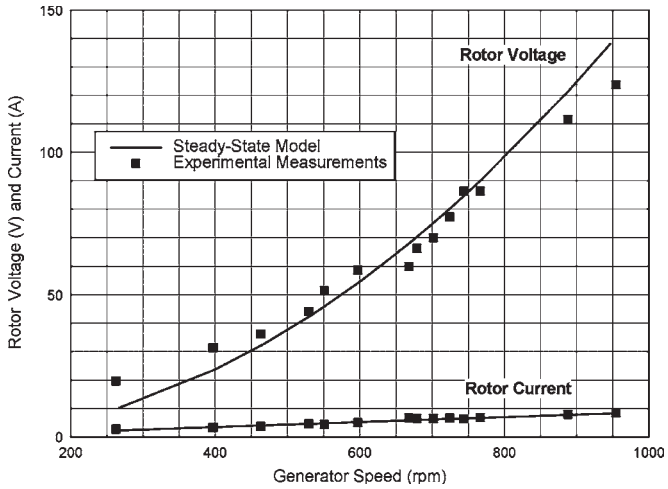

Fig. 7. Experimental results of 7.5-kW generator.

the DF connection. This particular operational feature is important and is due to the constraint that the airgap flux is maintained below the rated value to avoid overfluxing the machine. In this case, as the speed reduces, the rotor supply frequency reduces to keep the slip low, and as a result, the terminal voltage also reduces to avoid saturating the magnetizing paths in the generator.

Table IV summarizes the generated power, the rotor power factor at the generator terminals, and the efficiency. The values for the dynamic model match the steady-state values very closely, therefore, are omitted here for brevity. In this connection, the rotor converter is the only connection to the grid, and all the power is transferred through it while the grid-side inverter maintains unity power factor. The efficiencies are generally higher than those in the DF-connection mode, particularly if power-factor control is required, and reduce slightly as the speed reduces.

Fig. 7 illustrates the experimental results from the test generator connected in the IG mode and controlled using the real-time dynamic model described in the previous section. The correlation with the steady-state model results is on the whole very good. Table V summarizes the power, efficiency, and power-factor measurements, and again, these correlate well with the predicted results in Table IV.

TABLE V
IG MODE—7.5 kW—EXPERIMENTAL TEST RIG

Speed rpm	Grid Power W	Rotor Power Factor	Efficiency %
888.3	-1405.32	-0.55	92.28
767.4	-971.34	-0.55	90.79
744.1	-880.14	-0.55	90.20
724.8	-839.86	-0.55	90.00
702.2	-724.45	-0.54	88.64
679.7	-679.83	-0.54	85.07
668.2	-600.25	-0.51	84.25
597.7	-462.17	-0.54	93.22
529.6	-311.99	-0.52	90.17
398.1	-127.66	-0.41	83.26

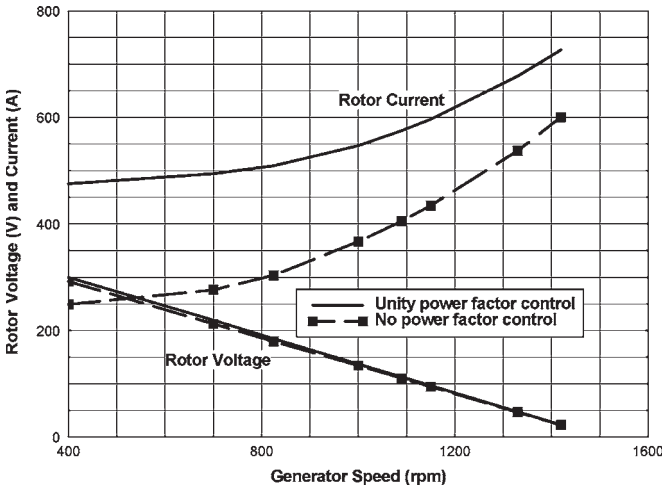

Fig. 8. Steady-state model of 2-MW generator.

VI. 2-MW COMMERCIAL WIND GENERATOR

The experimental results were performed on a small 7.5-kW laboratory test generator, and it would be unwise to scale any particular conclusion from those tests to a large commercial megawatt generator. For this reason, a theoretical study was performed on a 2-MW 690-V four-pole DF generator using the machine parameters provided by the manufacturer to make a realistic assessment of the benefits of the steady-state model and the proposed new IG-connection mode. There was no information relating to the rotor converter available, so it will be assumed that it would be rated typically to 30% of the generator, which equates to approximately 600 kVA.

Fig. 8 illustrates the rotor voltage and current for the DF connection using the steady-state algorithm, and as expected, the rotor voltage is largely controlled by the speed, and more rotor current is needed if the unity stator power factor is required. Furthermore, the maximum rotor current occurs close to synchronous speed (1500 r/min) where the amount of available wind power is the highest in this speed range. Tables VI and VII summarize the power, reactive power, and efficiencies with and without stator-power-factor control. Efficiencies are high in both cases, which is to be expected in higher power ratings, although, again, only copper losses have been included. There is a little significant reduction in the efficiency in this larger rating until the speed falls to 400 r/min or 73% slip.

TABLE VI
DF MODE—2 MW—STEADY-STATE EQUATIONS (NO pf CONTROL)

Speed rpm	Stator Power kW	Stator Power Factor	Grid Power kW	Rotor Reactive Power kVAr	Efficiency %
1420	-640.29	0.92	-604.20	338.84	99.39
1330	-562.00	0.90	-496.66	320.88	99.40
1150	-420.63	0.84	-321.30	310.45	99.40
1090	-378.02	0.81	-273.63	308.17	99.39
1000	-318.34	0.76	-211.32	305.75	99.36
825	-216.86	0.62	-118.59	290.86	99.21
700	-156.21	0.50	-72.31	290.96	98.95
400	-50.99	0.19	-13.07	293.23	95.60

TABLE VII
DF MODE—2 MW—STEADY-STATE EQUATIONS (pf CONTROL)

Speed rpm	Stator Power kW	Grid Power kW	Rotor Reactive Power kVAr	Efficiency %
1420	-640.55	-603.61	623.68	99.29
1330	-562.30	-496.09	622.07	99.29
1150	-420.92	-320.73	601.98	99.22
1090	-378.31	-273.06	599.76	99.18
1000	-318.62	-210.75	591.06	99.10
825	-217.15	-118.03	586.02	98.74
700	-156.50	-71.74	589.01	98.17
400	-51.26	-12.51	580.64	91.51

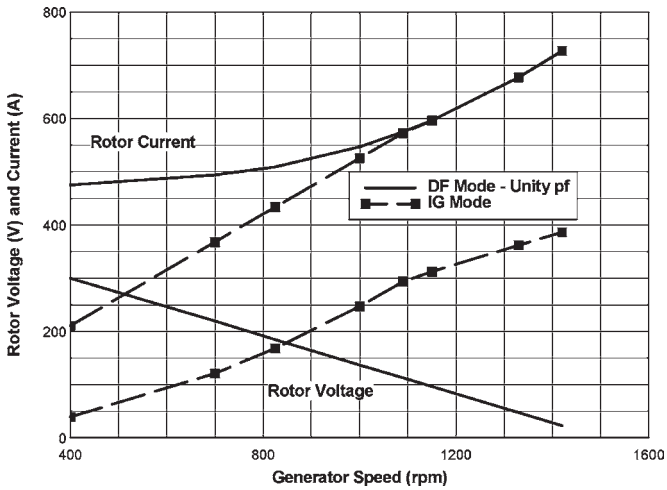

Fig. 9. DF- and IG-connection modes (steady-state model).

Fig. 9 illustrates the DF connection with power-factor control in direct comparison with the IG-connection mode. Again, it is evident that in the IG mode, the rotor voltage reduces as the speed reduces, and although the rotor currents are virtually identical at high speeds, the current falls away more significantly in the IG mode as the speed falls. Table VIII summarizes the grid power, rotor reactive power, and efficiency, and it is clear that there is a little difference in the efficiency until the speed falls to 400 r/min.

TABLE VIII
IG MODE—2 MW—STEADY-STATE MODEL

Speed rpm	Rotor Power kW	Rotor Reactive Power kVAr	Efficiency %
1420	-603.60	588.83	99.29
1330	-496.07	542.93	99.28
1150	-320.73	458.25	99.22
1090	-273.06	424.38	99.18
1000	-210.79	327.77	99.11
825	-118.25	184.13	98.92
700	-72.15	112.51	98.73
400	-13.37	21.00	97.78

The question therefore remains: What is the benefit of switching to the new IG-connection mode as the wind speed falls? The evidence in this section would suggest that the gains in output grid power are minimal in comparison to the DF connection with or without power-factor control. In fact, at higher speeds, the DF mode produces slightly more power. The benefits would therefore appear to lie in the rotor-converter ratings. The overall rating of the converter is related to the required speed range, which is typically 30% of the generator rating, as mentioned previously. However, the VA converter rating would be translated into maximum current and voltage ratings of the switching devices in the converter.

The device voltage rating is determined by the effective generator turns ratio, which relates the rotor voltage to the stator or grid voltage. In the steady-state model, however, the equivalent-circuit model uses referred rotor voltages, so the maximum operational rotor voltage for 30% slip would correspond to approximately 120 V. Fig. 8 confirms that this would equate to a minimum speed of 1050 r/min in the DF-connection mode.

The limiting factor therefore for operation at low speeds in the DF-connection mode is the rotor voltage, even if the available wind power is low. The rotor voltage is determined largely by the rotor slip. This is not the case in the IG mode where it is evident from the figures in both 7.5-kW and 2-MW-generator cases that the rotor voltage reduces as the speed reduces. The rotor voltage in this case is determined essentially by the converter supply frequency, and this reduces as the speed reduces. Fig. 9 clearly indicates that operation below approximately 700 r/min would only be possible in the IG connection without exceeding the voltage and current ratings of the rotor converter. In this particular example, there appears to be an operational gap between 1050-r/min DF mode and 750-r/min IG mode where the rotor voltage exceeds the estimated voltage limit. However, this is a theoretical study on a 2-MW generator, and the operating speed range was assumed to be 30% above and below synchronous speed. It would be a simple design exercise to ensure that in practice, the operational speed range could be extended seamlessly using the proposed IG-connection mode.

Another possible area where the IG-connection mode may have potential benefits is fault ride-through. There is a significant concern at the moment about protecting the rotor converter in the event of a sag or dip in the grid voltage at the stator terminals when the generator is connected in the DF mode. The present practice is to simply crowbar the connection between the converter and the rotor terminals. An alternative strategy might be to switch to the IG connection when a voltage sag or dip is detected. The rotor converter would then have full control of all power and reactive power flow through the generator.

In both cases, the economic benefits of implementing the IG-connection mode needs to be counterbalanced by the costs of the additional switchgear associated with the switching sequences of grid disconnection and synchronization before grid reconnection. Solid-state switches would be a practical solution if rapid grid disconnection/reconnection transitions were necessary.

VII. CONCLUSION

There is presently a significant interest in large offshore wind turbines up to 5 MW. One of the preferred options for these large turbines is the DF slip-ring generators that offset the cost of the rotor converter against a reduced operating speed range. Turbine manufacturers have proposed an operating scheme for low wind speeds that is claimed to improve the overall energy extraction and extend the operating speed range at which useful power can be extracted from the wind. The proposed operating scheme is to use a DFIG for normal wind conditions, but as the wind speed falls, the stator disconnects from the grid and short circuits it. The generator then reverts to a conventional IG mode of operation with all the power channeled through the rotor-side converter to the grid. Steady-state equivalent-circuit models have been developed to examine the performance benefits of both connections, and these have been validated against a practical real-time control scheme and also in laboratory experimental results on a small 7.5-kW generator. These have illustrated the significance of rotor voltage rating on the performance benefits. The DF-generator connection can be controlled to maintain close-to-unity power factor down to low wind speeds, but its operational speed limit is determined by the rising rotor voltage that increases with slip. Switching to the new single-sided connection (IG mode) still maintains unity power factor but allows the speed to reduce further, extracting more energy from the wind because the rotor voltage is now reducing as the speed reduces. The steady-state models for both DF- and IG-connection modes have been shown to be useful and accurate design tools for large wind-turbine operation in low-wind-speed conditions.

ACKNOWLEDGMENT

This paper is published with the approval of FKI Energy Technology, current owners of the wind-turbine manufacturer DeWind.

REFERENCES

[1] R. Datta and V. T. Ranganathan, "Variable-speed wind power generation using doubly fed wound rotor induction machine—A comparison with alternative schemes," *IEEE Trans. Energy Convers.*, vol. 17, no. 3, pp. 414–421, Sep. 2002.

[2] S. Müller, M. Deicke, and R. W. De Doncker, "Doubly fed induction generator systems for wind turbines," *IEEE Ind. Appl. Mag.*, vol. 8, no. 3, pp. 26–33, May/Jun. 2002.

[3] B. Rabelo and W. Hofmann, "Optimal active and reactive power control with the doubly-fed induction generator in the MW-class wind-turbines," in *Proc. Int. Conf. Power Electron. and Drive Syst.*, Oct. 22–25, 2001, vol. 1, pp. 53–58.
[4] L. Holdsworth, X. G. Wu, J. B. Ekanayake, and N. Jenkins, "Comparison of fixed speed and doubly-fed induction wind turbines during power system disturbances," *Proc. IEE—Generation, Transmiss. Distrib.*, vol. 150, no. 3, pp. 343–352, May 2003.
[5] L. Xu and W. Cheng, "Torque and reactive power control of a doubly fed induction machine by position sensorless scheme," *IEEE Trans. Ind. Appl.*, vol. 31, no. 3, pp. 636–642, May/Jun. 1995.
[6] E.-H. Kim, J.-H. Kim, and G.-S. Lee, "Power factor control of a doubly fed induction machine using fuzzy logic," in *Proc. 5th Int. Conf. Electr. Mach. and Syst.*, Aug. 18–20, 2001, vol. 2, pp. 747–750.
[7] S. Peresada, A. Tilli, and A. Tonielli, "Indirect stator flux-oriented output feedback control of a doubly fed induction machine," *IEEE Trans. Control Syst. Technol.*, vol. 11, no. 6, pp. 875–888, Nov. 2003.
[8] B. Hopfensperger, D. J. Atkinson, and R. A. Lakin, "Stator-flux-oriented control of a doubly-fed induction machine with and without position encoder," *Proc. IEE.—Electr. Power Appl.*, vol. 147, no. 4, pp. 241–250, Jul. 2000.
[9] M. Yamamoto and O. Motoyoshi, "Active and reactive power control for doubly-fed wound rotor induction generator," *IEEE Trans. Power Electron.*, vol. 6, no. 4, pp. 624–629, Oct. 1991.
[10] *The Carbon Trust & DTI Network Impact Study Annex 3: Distribution Network Topography Analysis*, Carbon Trust & DTI, London, U.K., Nov. 2003, pp. 52–53.
[11] R. Pena, J. C. Clare, and G. M. Asher, "Doubly fed induction generator using back-to-back PWM converters and its application to variable-speed wind-energy generation," *Proc. IEE.—Electric Power Appl.*, vol. 143, no. 3, pp. 231–241, May 1996.
[12] R. W. De Doncker, "The universal field oriented controller," *IEEE Trans. Ind. Appl.*, vol. 30, no. 1, pp. 92–100, Jan./Feb. 1994.
[13] E. Y. Y. Ho and P. C. Sen, "Decoupling control of induction motor drives," *IEEE Trans. Ind. Electron.*, vol. 35, no. 2, pp. 253–262, May 1988.
[14] R. D. Lorenz, "Tuning of field-oriented induction motor controllers for high-performance applications," *IEEE Trans. Ind. Appl.*, vol. IA-22, no. 2, pp. 293–297, Mar./Apr. 1986.

Alexander C. Smith (M'89–SM'02) received the B.Sc. Eng. and Ph.D. degrees from Aberdeen University, Aberdeen, U.K., in 1977 and 1980, respectively.

He had academic appointments at Imperial College (1983–1990) and Cambridge University (1990–1997). In 1997, he joined Invensys Brook Crompton (formerly Brook Crompton) as Head of Research responsible for motor technology. In 2000, he was appointed Senior Lecturer at the University of Manchester Institute of Science and Technology, Manchester, U.K., and Reader in Electrical Machines in 2002. In 2004, he was appointed Director of the Roll-Royce University Technology Center on Electrical Systems for Extreme Environments at the University of Manchester. He is currently with the School of Electrical and Electronic Engineering, University of Manchester.

Dr. Smith is a member of the Institute of Engineering and Technology [formerly Institution of Electrical Engineers, U.K. (IEE)], and past Chairman of the IEE Professional Network—Power Conversion and Applications.

Rebecca Todd received the M.Eng. degree in electrical and electronic engineering from the University of Manchester Institute of Science and Technology, Manchester, U.K., in 2001. She is currently working toward the Eng.D. degree at the University of Manchester, Manchester, U.K.

Mike Barnes (M'96) received the B.Eng. degree in engineering and the Ph.D. degree from the University of Warwick, Warwick, U.K., in 1993 and 1998, respectively.

He is currently a Senior Lecturer with the University of Manchester (formerly University of Manchester Institute of Science and Technology), Manchester, U.K. His principal research interests are in power electronics applied to machine drives and power systems.

Dr. Barnes is a member of the Institution of Electrical Engineers, U.K.

Peter J. Tavner received the M.A. degree in engineering sciences from Cambridge University, Cambridge, U.K., in 1969 and the Ph.D. degree from Southampton University, Southampton, U.K., in 1978.

He is currently a Professor of new and renewable energy in the School of Engineering, University of Durham, Durham, U.K. He has held a number of research and technical positions in industry including Technical Director of Laurence, Scott and Electromotors, Ltd. and Brush Electrical Machines, Ltd. Most recently, he has been the Group Technical Director of FKI Energy Technology. His research interests are in electrical machines for the extraction of energy from renewable sources and their connection to electricity systems. He retains a particular interest in electromagnetic analysis, the application of condition monitoring to electrical systems, and the use of converters with electrical machines.

Dr. Tavner is a winner of the Institution Premium of the Institution of Electrical Engineers, U.K.